Transcriptome Analysis of Arbuscular Mycorrhizal Roots during Development of the Prepenetration Apparatus[1][W]

Valeria Siciliano, Andrea Genre, Raffaella Balestrini, Gilda Cappellazzo, Pierre J.G.M. deWit, and Paola Bonfante*

Dipartimento di Biologia Vegetale, Università di Torino and Istituto Protezione Piante-CNR, 10125 Torino, Italy (V.S., A.G., R.B., G.C., P.B.); and Laboratory of Phytopathology, Wageningen University, 6709 PD Wageningen, The Netherlands (P.J.G.M.d.)

Information on changes in the plant transcriptome during early interaction with arbuscular mycorrhizal (AM) fungi is still limited since infections are usually not synchronized and plant markers for early stages of colonization are not yet available. A prepenetration apparatus (PPA), organized in epidermal cells during appressorium development, has been reported to be responsible for assembling a trans-cellular tunnel to accommodate the invading fungus. Here, we used PPAs as markers for cell responsiveness to fungal contact to investigate gene expression at this early stage of infection with minimal transcript dilution. PPAs were identified by confocal microscopy in transformed roots of *Medicago truncatula* expressing green fluorescent protein-HDEL, colonized by the AM fungus *Gigaspora margarita*. A PPA-targeted suppressive-subtractive cDNA library was built, the cDNAs were cloned and sequenced, and, consequently, 107 putative interaction-specific genes were identified. The expression of a subset of 15 genes, selected by reverse northern dot blot screening, and five additional genes, potentially involved in PPA formation, was analyzed by real-time reverse transcription-polymerase chain reaction and compared with an infection stage, 48 h after the onset of the PPA. Comparison of the expression profile of *G. margarita*-inoculated wild type and the mycorrhiza-defective *dmi3-1* mutant of *M. truncatula* revealed that an expansin-like gene, expressed in wild-type epidermis during PPA development, can be regarded as an early host marker for successful mycorrhization. A putative *Avr9/Cf-9* rapidly elicited gene, found to be up-regulated in the mutant, suggests novel regulatory roles for the DMI3 protein in the early mycorrhization process.

Arbuscular mycorrhizal (AM) symbiosis represents a unique interaction between a symbiotic fungus and its host plant. The fungus, an obligate biotroph belonging to Glomeromycota (Schüßler et al., 2001), is provided by the host plant with carbon sources required to complete its life cycle, whereas it facilitates the plant with the uptake of nutrients, such as phosphate (Smith and Read, 1997). Cellular, physiological, biochemical, and molecular research on mycorrhization is currently performed in many laboratories because positive effects of symbiotic fungi on the metabolism of their host plants are recognized as being beneficial to many ecosystems.

The AM-plant associations are a result of a long coevolutionary process (Karandashov and Bucher, 2005) that required profound morphological readjustments in the plant to accommodate the fungus and to facilitate the exchange of nutrients between the two partners. In both epidermal and cortical cells, the fungus is surrounded by a membrane of host origin. The formation of this apoplastic interface causes a dramatic structural re-organization of the plant cells with all their organelles (Bonfante, 1984; Bonfante and Perotto, 1995).

Development of new technological (in vivo confocal microscopy) and molecular (transformed plants expressing GUS or GFP markers) tools have allowed us to provide a clearer description of the sequence of events leading to a functional AM-plant association. By using a GFP-tag approach, Lohse et al. (2005) showed that arbuscular branches are surrounded by mitochondria and plastids, which are interconnected in a matrix, thereby confirming previously published electron microscopic images (Bonfante and Perotto, 1995) with new three-dimensional pictures. Genre et al. (2005) followed early cellular plant responses during initial AM colonization in roots of GFP-labeled *Medicago truncatula*. They discovered that epidermal cells of the host assemble an intracellular structure, required for the construction of an interface compartment, just below a fully developed fungal appressorium prior to penetration of the host. About 4 to 5 h after the development of an appressorium, cellular events strictly coordinated by the nucleus lead to the development of a prepenetration apparatus (PPA) that consists of a cytoplasmic column containing microtubule and microfilament bundles, very dense endoplasmic reticulum (ER) cisternae, and a central membranous

[1] This work was supported by Italian MIUR (Prin 2006; Cebiovem 2004–06), University of Torino (60% Project, 2004–06), and IPP-CNR (Biodiversity National Project) to P.B.

* Corresponding author; e-mail p.bonfante@ipp.cnr.it; fax 390116705962.

The author responsible for distribution of materials integral to the findings presented in this article in accordance with the policy described in the Instructions for Authors (www.plantphysiol.org) is: Paola Bonfante (p.bonfante@ipp.cnr.it).

[W] The online version of this article contains Web-only data.
www.plantphysiol.org/cgi/doi/10.1104/pp.107.097980

thread. Only after the column has been formed, the fungus grows across the cell within the newly formed membrane tunnel. The formation of a PPA suggests that the plant keeps major control over AM symbiosis development. This is reminiscent of infection thread formation, facilitating the entry of rhizobia in legume root hairs that guide them into the root cortex (Smith et al., 2006). Little is known about the molecular events during PPA formation. Genre et al. (2005) demonstrated that *MtENOD11* is specifically expressed before and during PPA formation. Recently, a more comprehensive picture of differential gene expression during AM-plant interactions has been achieved by analyzing cDNA libraries based on suppressive-subtractive hybridization (SSH; Wulf et al., 2003; Brechenmacher et al., 2004; Weidmann et al., 2004), cDNA AFLP profiles (Kistner et al., 2005), and cDNA arrays (Liu et al., 2003; Guimil et al., 2005; Hohnjec et al., 2005; Massoumou et al., 2007). cDNA arrays are only available from model plants like *Oryza sativa* and *M. truncatula*. However, detailed information on the initial stages of AM-plant interaction is still very limited, mainly due to the fact that it is extremely difficult to obtain synchronized colonization of roots by AM (Weidmann et al., 2004).

The discovery of the PPA enabled us to study differential gene expression closely associated with this structure that now could be used as a cellular marker during sampling of root fragments used to produce a SSH cDNA library. Here, we report on the differential expression of 15 genes that we confirmed by reverse northern dot blot analysis. The expression profile of these genes was also analyzed in *dmi3-1* mutant *M. truncatula* roots. The latter lacks a Ca^{2+}/calmodulin-dependent protein kinase that is required for the establishment of a functional AM-plant association (Levy et al., 2004) and the formation of a PPA (Genre et al., 2005).

Our data demonstrate that at least two novel genes are specifically up-regulated during the formation of PPA when compared with the control and the *dmi3-1* mutant. One of them encodes an expansin-like protein preferentially expressed in epidermal cells in contact with an appressorium. In addition, a gene coding for a putative *Avr9/Cf-9* rapidly elicited protein 264 (*ACRE264*) was found to be up-regulated in the *dmi3-1* mutant, suggesting that it is suppressed by DMI3 to possibly facilitate fungal entry into the host plant. The results of our findings are discussed in the light of beneficial and pathogenic plant-fungus interactions.

RESULTS

Confocal Microscopy of the AM-Plant Association

Confocal microscopic observations of ER organization in wild-type epidermal cells showed that PPA assembly in *M. truncatula* is not only triggered by the AM fungus *Gigaspora gigantea*, as reported by Genre et al. (2005), but also by *Gigaspora margarita*. There is a strict correlation between appressorium development and the formation of PPA in the epidermal cell below the appressorium (Fig. 1, A and B). In short, most epidermal cells in contact with an appressorium (stage 1) showed responses related to PPA assembly. They ranged from the formation of large ER patches to nuclear positioning at the appressorium contact site, to subsequent nuclear migration across the cell lumen associated with the development of a trans-cellular column of ER connecting the nucleus and the fungal contact site (Fig. 1, A and B).

However, epidermal cells of transformed roots derived from the *dmi3-1* mutant showed only nuclear repositioning without any sign of PPA assembly (Fig. 1D).

Observations made on the wild type 48 h after appressorium development (stage 2) showed that hyphae of *G. margarita* had already crossed the epidermis and reached the outer cortical cell layers. At this stage, epidermal cells no longer showed PPA structures (Fig. 1C), confirming they are transient in nature (Genre et al. 2005). In *dmi3-1* mutants, the fungus never penetrated the root epidermis.

Establishment and Characterization of a Subtractive cDNA Library

Quantity and quality of total RNA extracted from noninoculated and inoculated wild-type root segments collected during appressorium development (stage 1) were estimated by the 2100 AGILENT bioanalyzer. RNA integrity number values between seven and nine ensured the quality of the sample, while contamination of RNA by genomic DNA was excluded by showing the absence of any DNA peak eluting in front of 28S rRNA.

To establish an EST library enriched in plant genes induced in PPA developing cells, a SSH cDNA library was constructed consisting of 229 clones, of which 131 were selected at random, sequenced, and assembled in contigs, leading to the identification of 107 ESTs corresponding to putative *M. truncatula* genes up-regulated in *G. margarita*-inoculated roots. The cDNA inserts showed an average length of 438 bp (± 119 bp).

In Silico Analysis of ESTs

ESTs were analyzed with BLASTX and TBLASTX in the National Center for Biotechnology (NCBI) database and The Institute for Genomic Research (TIGR) MtGI (*M. truncatula* gene index) database, respectively. Most ESTs showed significant sequence similarities to plant genes, and for only a few no function or homology could be assigned. Unique sequences were deposited in the NCBI (or EMBL) database (accession nos. EC366174–EC366280; Supplemental Table S1). Sequences were functionally annotated using the annot8r_BLAST2GO program on the basis of the three organizing principles of the Gene Ontology database: molecular function, cellular component, and biological

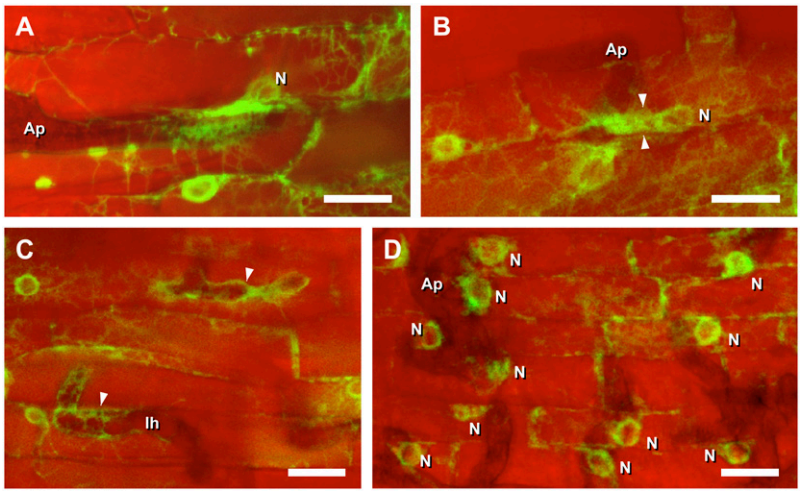

Figure 1. Confocal microscopic images of the wild type and *dmi3-1* mutant of *M. truncatula* root epidermal cells colonized by *G. margarita*. Bright-field images (red color) are superimposed on the optical sections showing GFP-HDEL localization (green color) in the ER. Plant nuclei (N), surrounded by dense ER, can be easily recognized. Due to their partial opaqueness, appressoria (Ap) and intracellular hyphae (Ih) are visible as dark areas in the bright-field image. A, PPA initiation in a wild-type epidermal cell contacted by an appressorium; the plant nucleus locates in the vicinity of the contact site, surrounded by a dense patch of ER. B, A complete PPA (arrowheads) has developed in a wild-type epidermal cell, connecting the appressorium contact site with the nucleus. C, Intracellular hypha traversing wild-type epidermal cells. PPAs have disappeared and a thin layer of ER (arrowheads) surrounding the fungus is visible. D, Epidermal cells of *dmi3-1* mutant roots showing nuclear repositioning at the appressorium contact sites, but no initiation of PPA assembly is visible. Bar = 30 μm.

process. The most frequently represented gene categories coded for enzymes or proteins with affinity for other (macro)molecules or proteins with putative catalytic or binding activities and involved in physiological processes in the intracellular compartment (Supplemental Fig. S1).

Sequence Selection and Primer Design

The cDNA clones were screened and selected by reverse northern dot blotting using cDNA smart probes from inoculated and noninoculated wild-type roots (stage 1) obtained as described above. Among the sequenced SSH clones, 15 sequences with the strongest hybridization signals were selected for real-time reverse transcription (RT)-PCR (data not shown). Similarities with known plant proteins as well as the presence of one or more conserved functional domains were detected in these selected genes (Supplemental Table S2). In addition, targeted genes expected to be involved in PPA development were chosen, including cytoskeleton-related genes (*α-tubulin*, *β-tubulin*, *actin*), a secretion marker (*Golgi SNARE11*), and, finally, *DMI3*, known to be involved in the symbiosis pathway (Levy et al., 2004). Primer pairs corresponding to these sequences were designed (Table I).

The absence of cross-hybridization with fungal templates was verified for each primer pair by performing PCR on genomic DNA of *G. margarita*. No amplification products were obtained from *G. margarita* DNA, confirming that all selected genes were of plant origin (data not shown).

Expression Profiling of Fungus-Induced Genes in Wild-Type Genotype

Real-time RT-PCR was carried out to verify mRNA expression levels for the two sets of genes described above (one resulting from the SSH library and the other representing the set of targeted genes). New samples were collected from inoculated and noninoculated wild-type roots at stages 1 and 2 and from *dmi3-1* roots at stage 1 (Table II).

Results shown in Figure 2, Table II, and Supplemental Figure S2 are presented as ratios between the relative expression level of each gene in inoculated and noninoculated roots. In the wild type, the up-regulation of 10 SSH sequences compared to noninoculated roots at stage 1 could be confirmed (Table II; Fig. 2, A–J). They include sequences encoding a putative cellulose synthase (*Cel synt*; Fig. 2A), a putative expansin-related protein 1 precursor (*Exp-like*; Fig. 2B), a putative receptor-like protein kinase (*RK20-1*; Fig. 2C), an 1-aminocyclopropane-1-carboxylic acid oxidase (*ACO*; Fig. 2D), a putative resistance protein (*KR1*; Fig. 2E), a pathogenesis-related (PR) protein (*PR10*; Fig. 2F), a nonsymbiotic hemoglobin (*non-sym-Hb*; Fig. 2G), a putative nodulin-like protein (*Nod-like*; Fig. 2H), a putative unknown protein similar to K07C11.4 (*K07C11.4*; Fig. 2I), and a putative *O*-linked *N*-acetyl glucosamine transferase (*OGT*; Fig. 2J). Four additional sequences encoding proteins with similarity to a cationic peroxidase (*CP*; Fig. 2K), a pectin-glucuronyltransferase-like (*pectin-GUT-like*; Fig. 2L), *ACRE264* (Fig. 2M), and a seed protein precursor (*SPP*; Fig.

Table I. *Sequences selected for real-time PCR and corresponding primer pairs*

NCBI Gb or TIGR TC accession numbers as well as specific primers and annealing temperatures are reported for each sequence. Abbreviations used in text are in parentheses. Top, SSH-derived genes. Bottom, Targeted ESTs.

Accession No.	TBLASTX Annotation at TIGR MtGI	Forward Primer	Reverse Primer	Annealing Temperature
				°C
NCBI Gb				
EC366238	*Cellulose synthase* (*Cel synt*)	ATGAGCTCAATGGAGGAGGA	AGCAATGGAATGGAGGATTG	60
EC366239	*Expansin-related protein 1 precursor* (*Exp-like*)	GTCGGTCTTATGGGGCAGTA	ATTGCGAACCTTGACTCCAC	60
EC366226	*Receptor-like protein kinase RK20-1* (*RK20-1*)	CAAAACTGGCTTCGCATCTC	ATCAGCAGCAACAACACGAC	60
EC366186	*Aminocyclopropane carboxylic acid oxidase* (*ACO*)	GCCGAGGTACCAGAATTTGT	TTGTCGCAGTAATGACCAGG	60
EC366187	*Resistance protein KR1* (*KR1*)	GCAGCCGATCCAATAGTCTC	TTCACCAATCCTTGCAACTG	60
EC366218	*PR 10 protein* (*PR10*)	AAGCTTTGCAATGGATCCTC	CAGCATAGTTGGTGGTGGTG	60
EC366224	*Nonsymbiotic hemoglobin* (*non-sym-Hb*)	GGTGAAGTCATGGAATGCAA	TTTTTGAGCTGATGGAGCAA	60
EC366236	*Nodulin-like protein* (*Nod-like*)	AGTGGAACCACTGAGCCAAC	AGAAACTAGCCCAACCACCA	60
EC366248	*K07C11.4 protein* (*K07C11.4*)	TAAACACACGGCCAAAGTCA	CTTCCTGCTGCAATTGATGA	60
EC366214	*O-linked N-acetyl glucosamine transferase* (*OGT*)	CTGCACCAGTCCAAGTTTCA	AAGTAGCAATGCGGGAGATG	60
EC366200	*Cationic peroxidase* (*CP*)	GAGGCATACCTTCCTGACCA	CAAGCAAAGCAACAACTCCA	60
EC366257	*Pectin-glucuronyltransferase-like* (*pectin-GUT-like*)	CAGTGTGCTCCCCAAGCTAT	TACGATGACCAGCCCAAAAT	60
EC366179	*Avr9/Cf-9 rapidly elicited protein 264* (*ACRE264*)	GGTTATGCGGCTCCTGAGTA	CCATTCCACCAAGTTTTTCC	60
EC366175	*Seed protein precursor* (*SPP*)	TGTTGTCGCATTGACTTGGT	AACGCAGTGATGTGCCATAG	60
EC366255	*Mitogen-activated protein kinase* (*MAPK*)	GCTCCTCCGATAGTGCTTGA	TCGCCATATGGATCATGAAA	60
TIGR TC				
TC101291	*Golgi SNARE11*	ATTTGGAAGAGGGTGGAGGT	AAAAGTCGAACGCTGGAAGA	59
TC106341	*β-Tubulin*	ACTTATTGATTCAGTTCTCGA	TCCAGATCCCGTTCCTCCTC	55
TC100406	*α-Tubulin*	GAGAGTGCATTTCAGTTCACA	CTTTCCAGCACCGGTCTCAC	57
TC107326	*Actin*	CGTATGAGCAAGGAGATCAC	CCTCCAATCCAGACACTGTA	56
TC101847	*DMI3*	TCATTGATCCCTTTTGCTTCTCGT	GATGCTACTTCCTCTTTGCTGATGC	60
TC106518	*Glyceraldehyde phosphate dehydrogenase* (*GAPDH*)	GCTAGCACTGGTGCTGATATT	TTCCTTCTCATTGACACCAAC	60

2N) were also up-regulated but to a lower level, while only a mitogen-activated protein kinase-encoding gene (*MAPK*; Fig. 2O) showed a weak down-regulation (ratio lower than 1) in the inoculated roots. During stage 2 (Table II; Supplemental Fig. S2), only four of these genes (*KR1*, *K07C11.4*, *OGT*, and *SPP*) were up-regulated beyond the 2-fold threshold in inoculated versus noninoculated roots. Among the targeted genes (Table II; Fig. 2, P–S; Supplemental Fig. S2), *SNARE11* and *β-tubulin* were up-regulated in both stages (Fig. 2, P and Q; Supplemental Fig. S2), while *α-tubulin* and *actin* showed an expression level just below 2 (Fig. 2, R and S; Supplemental Fig. S1). The *DMI3* gene was clearly up-regulated during stage 1 but not at stage 2 (Supplemental Fig. S1).

When the results presented in Figure 2 and Supplemental Figure S2 are compared, eight sequences (*Cel synt*, *Exp-like*, *RK20-1*, *ACO*, *PR10*, *non-sym-Hb*, *Nod-like*, and *DMI3*) appear to be exclusively up-regulated during stage 1 (Table II).

Expression Profiling of Fungus-Induced Genes in the *dm3-1* Mutant

The expression profiles of the selected genes were also followed in the *dmi3-1* mutant (Table II; Fig. 2). Only stage 1 was investigated, as in our experimental setup the *dmi3-1* mutant never showed intraradical colonization. Eleven sequences were more than 2-fold up-regulated in inoculated roots, including *Cel synt* (Fig. 2A), *RK20-1* (Fig. 2C), *ACO* (Fig. 2D), *KR1* (Fig. 2E), *PR10* (Fig. 2F), *non-sym-Hb* (Fig. 2G), *OGT* (Fig. 2J), *pectin-GUT-like* (Fig. 2L), *ACRE264* (Fig. 2M), *SNARE11* (Fig. 2P), and *β-tubulin* (Fig. 2Q). *K07C11.4* was slightly down-regulated (Fig. 2I), whereas *SPP* was strongly down-regulated (Fig. 2N). The remaining genes (Fig. 2, B, H, K, O, R, and S), showed only slightly higher expression in inoculated compared to noninoculated roots (ratio between 1 and 2). As expected, no *DMI3* transcript was detected in the *dmi3-1* mutant roots (data not shown).

The expression profiles of inoculated wild-type and *dmi3-1* roots were compared for significance in an

Table II. *Expression profiling of selected sequences*

Real-time RT-PCR results of the sequences selected by reverse northern dot blot (top) and additional targeted genes (bottom). Columns A, B, and C give approximated ratios of: (A) wild-type stage 1 (WT_1) versus wild-type control (WT_C), (B) wild-type stage 2 (WT_2) versus wild-type control, and (C) *dmi3-1* mutant stage 1 (*dmi3-1*$_1$) versus *dmi3-1* mutant control (*dmi3-1*$_C$). Exact expression levels and SDs can be found in Figure 2 and Supplemental Figure S1. Ratio values equal to or higher than 1 are shown as black circles (● ≥ 1, ●● ≥ 2, ●●● ≥ 3, etc.); ratio values lower than 1 are shown as white circles (○ < 1, ○○ ≤ 0.5, ○○○ ≤ 0.33, etc.). Diagrams schematize the different samples.

Sequences	Expression Profiling Ratios		
	(A) WT_1/WT_C	(B) WT_2/WT_C	(C) *dmi3-1*$_1$/*dmi3-1*$_C$
Cel synt	●●●	●	●●●
Exp-like	●●●●●●●●	●	●
RK20-1	●●	●	●●
ACO	●●	●	●●
KR1	●●	●●●	●●
PR10	●●	●	●●
Non-Sym-Hb	●●	●	●●
Nod-like	●●●	●	●
K07C11.4	●●●●●	●●●	○
OGT	●●	●●	●●●
CP	●	●	●
Pectin-GUT-like	●	●	●●
ACRE264	●	●	●●
SPP	●	●●●	○○○○
MAPK	○	●	●
SNARE11	●●	●●	●●
β-Tubulin	●●	●●	●●
α-Tubulin	●	●	●
Actin	●	●	●
DMI3	●●	●	–

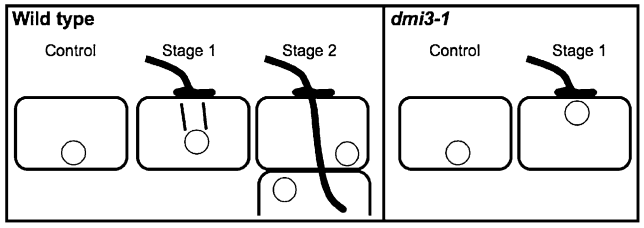

ANOVA test (Table II; Fig. 2). Eleven sequences revealed no statistically significant differences in the expression pattern between inoculated wild-type and *dmi3-1* roots (Fig. 2, A, C, D, E, F, G, K, P, Q, R, and S). The remaining sequences showed statistically significant differences ($P < 0.05$) in their expression in response to inoculation with *G. margarita* in a genotype-specific manner. Four showed decreased expression in inoculated *dmi3-1* roots when compared to inoculated wild-type roots (Fig. 2, B, H, I, and N). In contrast, the other four genes showed increased expression in mutant roots when compared to the wild type (Fig. 2, J, L, M, and O).

In conclusion, when the threshold for increased expression is set above 2-fold, only *Exp-like* and *Nod-like* show specific up-regulation in wild-type stage 1, compared to *dmi3-1* stage 1, while only *pectin-GUT-like* and *ACRE264* are specifically up-regulated in *dmi3-1* stage 1, compared to wild-type stage 1 (Table II; Fig. 2; Supplemental Fig. S2).

Localization of *Exp-like* Transcripts by in Situ Hybridization

As the *Exp-like* gene was significantly up-regulated in the early phase of infection, we set out to localize its corresponding transcripts by in situ hybridization with a ribosomal *18S* probe as a positive internal control. In inoculated wild-type roots, a significantly higher level of chromogenic signal was observed in epidermal cells during appressorium development compared to noninoculated control roots (Fig. 3, A and B, and inset). Control experiments with the sense probe never showed a significant signal (Fig. 3C).

DISCUSSION

In this study, we developed a targeted sampling method to study expression profiles of the *G. margarita-M. truncatula* association in a standardized way by using the presence of PPAs as a marker during sampling. In addition, we compared the transcript profiles of inoculated wild-type roots with the inoculated *dmi3-1* mutant roots. This led to the identification of genes whose expression is affected by the mutation in the *DMI3* gene. All these genes, some of which are reported here for the first time (to our knowledge), are potentially involved in early AM interactions since sampling preceded arbuscule development.

Expression Profiling of Genes in the Early Stages of the *M. truncatula-G. margarita* Interaction

To obtain further insight into the impact of appressorium formation and PPA presence on plant gene expression, we identified 107 ESTs corresponding to putative *M. truncatula* genes up-regulated during early contact with *G. margarita* (Supplemental Table S1). A few of these sequences had already been suggested to be AM regulated (Brechenmacher et al., 2004; Weidmann et al., 2004; Vieweg et al., 2004, 2005; Hohnjec et al., 2005), even if in studies performed on whole roots several weeks after inoculation. Following reverse northern dot blot hybridization, 15 out of 107 sequences were confirmed as significantly up-regulated in inoculated roots during stage 1, including genes reported to be involved in signal transduction (*RK20-1*), defense responses (*KR1*, *PR10*, *ACRE264*), and cell wall modification (*Cel synt*, *Exp-like*, *pectin-GUT-like*, and *CP*).

Genes with Expression Profiles Correlated with PPA Presence

In our experimental setup, we could assign some differentially expressed genes to the presence or absence of a PPA. Using real-time RT-PCR, we first

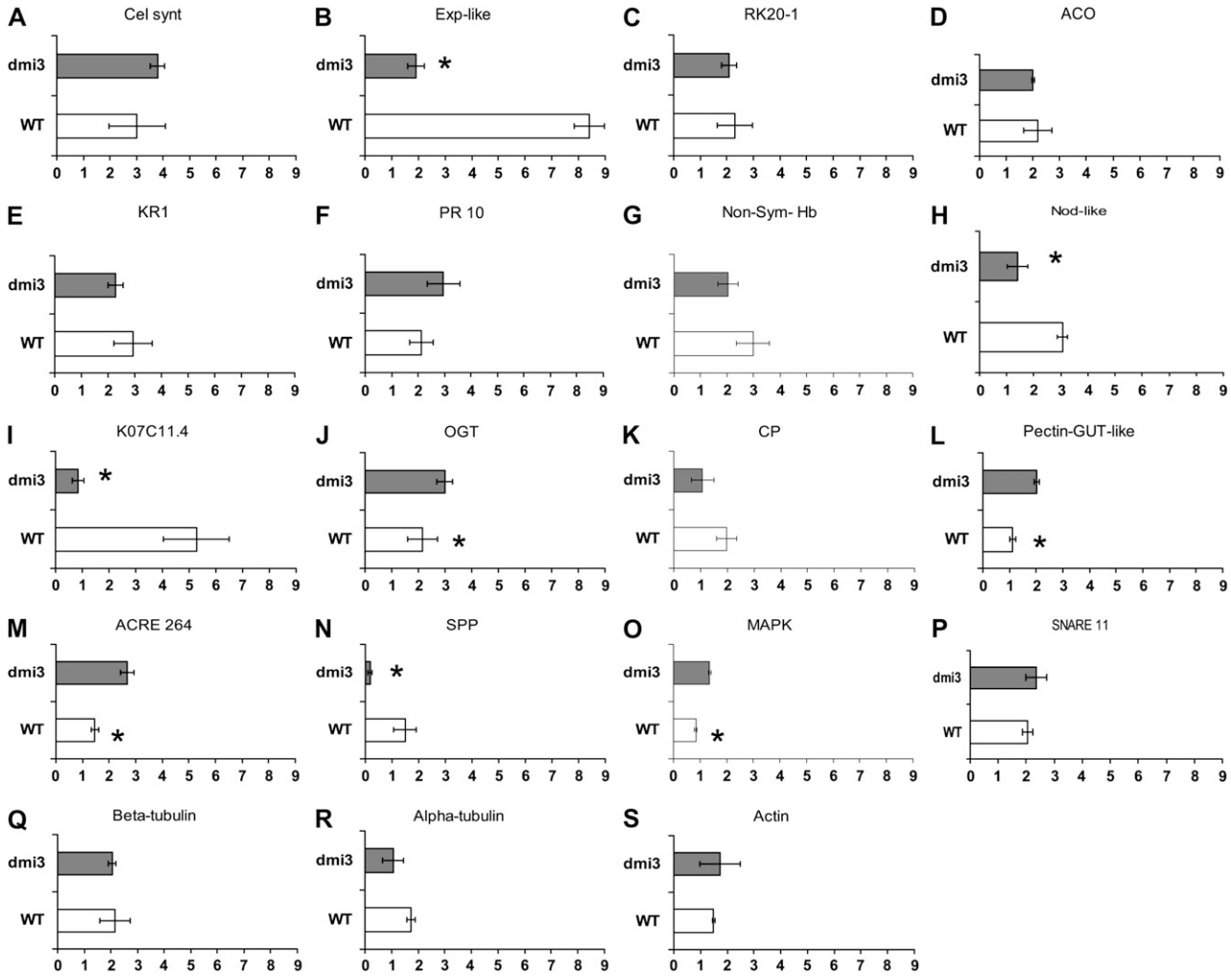

Figure 2. Transcript accumulation of selected sequences upon inoculation with *G. margarita* in wild-type (white bars) and *dmi3-1* mutant roots (gray bars) at stage 1. Bars indicate the ratio between mRNA levels in inoculated versus noninoculated root segments. Mean values are shown with SES from three independent root segment inoculations; asterisks (*) indicate statistically significant differences according to ANOVA test ($P < 0.05$).

demonstrated that 13 out of 20 genes were up-regulated (at least 2-fold) at the time point of appressorium and PPA development when compared to the noninoculated root controls (Table II). They include 10 SSH sequences and three targeted genes. The latter encode proteins involved in membrane fusion (*SNARE11*), cytoskeleton (*β-tubulin*), and AM signaling (*DMI3*, a Ca^{2+}/calmodulin-dependent protein kinase). These data extend results from macroarray hybridization studies (Manthey et al., 2004), where a β-tubulin (*MtTubb1*) appeared also to be up-regulated in fully colonized roots. Previous microscopic observations support these results, showing that the cytoskeleton reorganizes both prior to and during epidermal cell colonization (Genre and Bonfante, 2002; Genre et al., 2005). Similarly, although activation of genes involved in membrane proliferation and vesicle trafficking, such as *SNARE11*, has never been reported in the early stage of AM interactions, numerous Golgi bodies have been reported to occur in colonized cells (Balestrini et al., 1996), indirectly supporting our findings.

More interestingly, five out of 13 genes up-regulated during stage 1 remained up-regulated 48 h later (*KR1*, *K07C11.4*, *OGT*, *SNARE11*, *β-tubulin*; Table II), when PPA has already been disassembled and the fungus has reached the outer cortical layer (stage 2), suggesting that the remaining eight genes are specifically up-regulated in stage 1.

The expression of the latter genes (*Cel synt*, *Exp-like*, *RK20-1*, *ACO*, *PR10*, *non-sym-Hb*, *Nod-like*, and *DMI3*) seems specifically affected in the epidermal layer in contact with an appressorium that has induced a PPA structure in the host. A few of these genes seem to be associated with defense responses, like *PR10*. Up-regulation of genes involved in cell wall synthesis supports the hypothesis that, during the PPA development, cellulose synthase is required for preparation of the interface compartment (Balestrini et al., 1994;

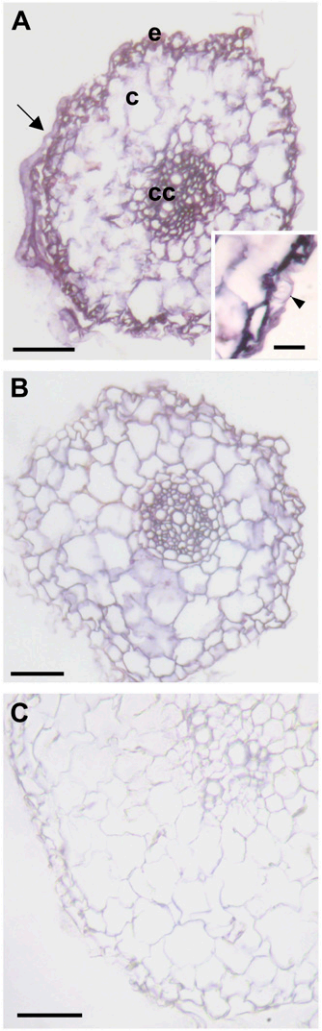

Figure 3. Localization of *Exp-like* mRNA in sections from differentiated regions of inoculated (A and C) and noninoculated (B) wild-type *M. truncatula* roots (stage 1) by cold in situ hybridization. A, In situ hybridization with DIG-labeled RNA *Exp-like* antisense probe. The chromogenic signal is most intense in the epidermal layer (e), in addition to vascular tissue (cc). A low hybridization signal is present in cortical cells (c). The arrow indicates the fungus in contact with the root. Bar corresponds to 50 μm. Inset, Magnification of epidermal cells. At higher magnification the presence of a strong hybridization signal is present in epidermal cells in contact with the fungus. The arrowhead indicates a transversally sectioned hypha. Bar corresponds to 10 μm. B, A low hybridization signal is present in all cell types of noninoculated root segments. Bar corresponds to 45 μm. C, No hybridization signal is observed in control root segments with the sense probe. Bar corresponds to 35 μm.

Balestrini and Bonfante, 2005; Genre and Bonfante, 2005). Interestingly, cellulose has also been detected in young infection threads (Rae et al., 1992). Finally, the activation of *DMI3* during stage 1 is of particular interest, as this gene is also preferentially expressed in root tissues and nodules as reported by Levy et al. (2004), but so far its up-regulation has not been reported during colonization of plants by AM fungi. However, Navazio et al. (2007) recently reported the up-regulation of its ortholog in soybean (*Glycine max*) cells 24 h after treatment with a cell-free culture medium of *G. margarita*. We therefore suggest that *DMI3* gene activation could be a rapid and transient response induced by a diffusible fungal factor or by appressorium contact, which supports the proposed role of the DMI3 protein as a mediator of calcium signals. The fact that up-regulation is probably limited in time and space also supports the observations by Tirichine et al. (2006), who observed only small changes in *DMI3* expression levels during nodulation when colonized tissue was analyzed.

The Mutation in the *DMI3* Gene Has a Profound Effect on *M. truncatula* Gene Expression

The role of *SYM* genes has been intensively studied in recent years. Parniske (2004) showed that they control legume symbioses (both AM and nodulation), while Kistner et al. (2005) demonstrated that the vast majority of genes induced by AM fungi in wild-type plants are not induced in roots of *Lotus japonicus* carrying independent mutations in each of seven *SYM* genes, indicating their requirement for transcriptional activation of downstream genes. Similarly, Weidmann et al. (2004) demonstrated that at least 11 *M. truncatula* genes were not activated in roots of the *dmi3-1* mutant by appressoria of *Glomus mosseae* or after treatment with diffusible fungal factors.

Our real-time RT-PCR data suggest that roughly three clusters of genes can be distinguished and located at different positions in the signaling pathway controlling root symbiosis, as described by Oldroyd et al. (2005). We found that eight out of the 13 genes differentially expressed during stage 1 in inoculated wild-type roots (Table II, A versus C) showed a similar expression pattern in *dm3-1* mutant roots, suggesting that they are either not governed by *SYM* genes or located upstream of *DMI3* (Levy et al., 2004). Interestingly, *M. truncatula RK20-1* is one of them. Lange et al. (1999) found that common bean (*Phaseolus vulgaris*) *RK20-1* is activated after Nod factor treatment or after pathogen inoculation, while its expression is unaffected 5 d after colonization by rhizobium or *G. mosseae*. This suggests that RK20-1 is induced by diffusible factors that are released by AM fungi during early stages of infection and is repressed when a symbiotic interaction has been established. Based on the different expression profiles in symbiotic and pathogenic interactions, one cannot exclude that RK20-1 might play a role also in the perception of a not yet identified diffusible fungal factor. The simultaneous activation of genes involved in cytoskeleton activity (α- and β-*tubulin*, *actin*) is remarkable since, even in the absence of a PPA in the *dmi3-1* mutant, nuclear movements have been reported (Genre et al., 2005) and have been confirmed in our study, suggesting that some residual perception and downstream signaling still occur in the *dm3-1* mutant.

The second cluster of genes shows lower expression in the *dm3-1* mutant than in the inoculated wild-type roots (Table II, A versus C). Proteins encoded by such genes might be located downstream of DMI3 in the

AM signal transduction pathway. Interestingly, this cluster includes *Exp-like* and *Nod-like*. Expansins are a superfamily of proteins that play a crucial role in cell wall loosening. An expansin-encoding gene is up-regulated in nitrogen-fixing nodules (Giordano and Hirsch, 2004) and a tomato (*Lycopersicon esculentum*) expansin gene (*LeEXPA5*) was recently found to be induced by a root-knot nematode during early stages of infection when plant cells expand to form the gall (Gal et al., 2006). Expansin genes have been reported to be up-regulated after infection of plants by AM fungi before (Journet et al., 2002; Liu et al., 2003; Weidmann et al., 2004). In addition, expansins have been observed to localize along the walls of mycorrhizal cells and in the interface matrix (Balestrini et al., 2005). *Exp-like* shows a weak homology with Arabidopsis (*Arabidopsis thaliana*) expansin-related protein 1 precursor possibly belonging to expansin-like B family. Even without knowing the precise function of the expansin-like B family (Sampedro and Cosgrove, 2005), it is expected that an increase in plant cell wall plasticity, triggered by fungal contact or by a diffusible fungal factor, is a prerequisite to accommodate the fungus in the plant. The demonstration by in situ hybridization that *Exp-like* transcripts accumulate in epidermal cells after fungal contact confirmed our real-time RT-PCR results. *Nod-like* encodes a putative membrane protein, based on in silico analysis in EST collections obtained from roots during nodulation and mycorrhization (http://www.tigr.org/tdb/e2k1/mta1/). Its activation in both types of beneficial interaction suggests it to be a molecular marker of early root responses during the onset of symbioses. Both genes are more strongly up-regulated in stage 1 than in stage 2 (Table II). Their limited up-regulation in the *dmi3-1* mutant (below 2-fold; Fig. 2, B and H) suggests that their regulation is only partially DMI3 dependent.

In addition, two sequences in this cluster (*K07C11.4* and *SPP*) have a lower expression level in inoculated compared to noninoculated *dmi3-1* mutant roots (Fig. 2, I and N), showing that they are actively down-regulated during fungal contact in the absence of the intact *DMI3* transcripts.

We also detected a third cluster of genes, which is up-regulated in *dmi3-1* mutant roots (Table II, A versus C). Most previous reports indicate that genes with an AM-dependent regulation are not up-regulated in the *dmi3-1* mutant (Weidmann et al., 2004). Only Amiour et al. (2006), using a proteomic approach, detected six putatively novel proteins in *dmi3-1* mutant roots during appressorium formation, but they have not yet been identified. In contrast, here we report for the first time (to our knowledge) that DMI3 can also inhibit transcription of some genes as their expression in stage 1 of inoculated *dmi3-1* roots is higher than in the same stage of inoculated wild-type roots (ANOVA test $P < 0.05$). They include *OGT*, *pectin-GUT-like*, and *ACRE264*. We can only speculate on their roles in symbiosis. *Pectin-GUT-like* activation might suggest the incorporation of pectin-like products in cell wall appositions as observed in roots of mycorrhiza-defective *L. japonicus* (Bonfante et al., 2000). The up-regulation of *ACRE264* in *dmi3-1* mutant roots (Fig. 2; Table II, A versus C) suggests that DMI3 might suppress this defense-related gene. *ACRE264* was initially reported to be up-regulated in tobacco (*Nicotiana tabacum*) cell suspensions expressing the *Cladosporium fulvum Cf-9* resistance gene, after treatment with the matching Avr9 elicitor. The gene that we found to be up-regulated in *dmi3-1* roots shows similarity to *ACRE264* and is now identified as a tomato protein kinase (ACK1) required for full resistance to *C. fulvum* strains expressing the *Avr9* gene (Rowland et al., 2005).

Discovery of a defense-related protein kinase gene whose expression is up-regulated in the early phase of an aborted AM fungus-plant association suggests that host defense responses need to be quenched during the PPA formation that is required to successfully accommodate the AM fungus. This also suggests that basal defense responses have to be kept under control not only in compatible plant-pathogen interactions but also in plant-symbiotic interactions as suggested by Dangl and Jones (2001).

CONCLUSION

Our targeted sampling method enabled us, on one hand, to avoid a dilution effect masking the detection

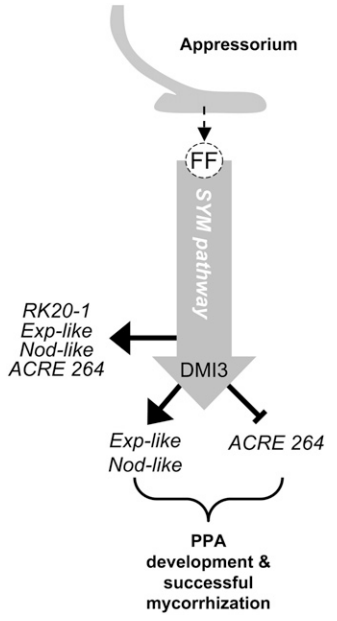

Figure 4. Diagram highlighting the role of DMI3 in a hypothetical gene expression pathway during PPA assembly in response to contact by the AM fungus. The SYM pathway, activated after perception of a putative diffusible fungal factor (FF), weakly up-regulates *Exp-like*, *Nod-like*, *ACRE264*, and *RK20-1* upstream of DMI3. DMI3 is required for up-regulation of *Exp-like* and *Nod-like* but represses the *ACRE264* gene. These two functions—absent in *dmi3-1* mutant—are most likely required for PPA development and establishment of a compatible AM fungus-plant interaction.

of locally and transiently expressed genes (Küster et al., 2007) and, on the other hand, to highlight genes activated during PPA development. Even with the limitations of our somewhat artificial system of transformed root organ cultures, we have not only gained a better understanding of the relation between appressorium perception and PPA formation, but also have identified new marker genes expressed during PPA development.

Based on our reported observations, we suggest that DMI3 may play a pivotal role in interpreting and modulating plant responses to early AM colonization (Fig. 4). On the one hand, its activity will boost the up-regulation of plant genes that are required for the accommodation of the AM fungus, such as *Exp-like* and *Nod-like*, which are already partially up-regulated upstream of DMI3. On the other hand, the Ca^{2+}/calmodulin-dependent kinase activity of DMI3 will suppress basal defense-related genes like *ACRE264*, possibly after perception of a diffusible fungal factor or merely after physical contact of the host with the fungal appressorium.

MATERIALS AND METHODS

Biological Material and Experimental Setup

Agrobacterium rhizogenes-transformed root cultures expressing the GFP-HDEL construct (see below) were derived from both wild-type *Medicago truncatula* 'Jemalong' A17 and mutant *dmi3-1* (TRV25; Sagan et al., 1998) and kindly provided by D. Barker (INRA/CNRS, Castanet Tolosan, France). The GFP-HDEL construct, where the GFP sequence is conjugated to a signal peptide and the tetra-peptide HDEL, is driven by the "constitutive" cauliflower mosaic virus 35S promoter and specifically labels the ER (Haseloff et al., 1997). Roots were cultured on square petri dishes containing M medium, according to Chabaud et al. (2002). Spores of *Gigaspora margarita* (BEG 34) were collected from pot cultures of mycorrhizal *Trifolium repens*, vernalized at 4°C for 2 weeks, and surface sterilized with 3% (w/v) chloramine T + 0.03% (w/v) streptomycin, according to Lanfranco et al. (2005). Spores were then placed in M medium in petri dishes and cultured at 30°C to induce germination.

The targeted AM inoculation technique developed by Chabaud et al. (2002) for studying the interaction between *Gigaspora* spp. and transformed roots of *M. truncatula* was chosen for the possibility it offers direct observation of colonization events and easy collection of samples.

Briefly, 10 to 12 germinated spores of *G. margarita* were transferred to petri dishes containing four to five growing *M. truncatula* root explants and positioned below the growing lateral roots, to facilitate reciprocal contacts. All root cultures were incubated at 26°C in the dark and vertically oriented. Root and hyphal growth was followed daily under a stereomicroscope. *G. margarita* spores germinated in 2 to 4 d; after inoculation, germ tubes grew upwards and branched, contacting root epidermis. Appressoria were generally observed after 5 d.

Confocal Microscopy

For confocal microscopy observations, root cultures were covered with 1 mL of sterile water, on top of which was laid a thin (25 μm) gas-permeable plastic film (bioFOLIE 25; Sartorius) as described by Genre et al. (2005).

Observations were performed directly in the petri dishes using a Leica TCS SP2 confocal microscope equipped with a long-distance 40× water-immersion objective (HCX Apo 0.80). The argon laser band of 488 nm was used to excite the GFP and an emission window at 500 to 525 nm was set for GFP fluorescence acquisition. Cell responses beneath fungal appressoria were observed in both genotypes at the moment of appressorium development (stage 1) and 48 h later (stage2). The spots where cell responses were detected were labeled with a marker on the bottom of the petri dish.

Sampling and RNA Extraction

The selected root segments, previously identified at the confocal microscope, were sampled under a stereomicroscope. Five- to 8-mm-long root pieces were excised from inoculated wild-type roots, directly beneath fungal appressoria at stage 1 and stage 2. Samples from inoculated *dmi3-1* roots were collected only at stage 1. Corresponding root segments were harvested as controls at each stage from noninoculated roots grown in the same conditions. Apical areas were always excluded. About 50 root segments were collected from each inoculation. Three independent inoculations were analyzed in each experiment. Root fragments sampled at stage 1 from inoculated and noninoculated wild-type roots were used for SSH library construction, reverse northern dot blot, and real-time RT-PCR analysis (see below), while stage 1 segments collected from *dmi3-1* roots and stage 2 segments collected from wild-type roots were only used for real-time RT-PCR analysis.

Samples were flash frozen in liquid nitrogen and stored at −80°C. RNA was extracted from inoculated and noninoculated root pieces, using the SV Total RNA Isolation System kit (Promega). All RNA samples were quantified and quality checked (integrity and absence of genomic DNA) by Agilent 2100 BIOANALYZER.

SSH Library Construction

The SSH library (Diatchenko et al., 1996) was constructed at stage 1 from GFP-HDEL wild-type root pieces collected beneath fungal appressoria and containing PPA forming cells (tester) and noninoculated segments (driver). Briefly, RNA from tester and driver were used as templates to synthesize two cDNA populations, which were PCR amplified with the BD SMART PCR cDNA synthesis kit (BD Biosciences), according to Cappellazzo et al. (2007). Thereafter, cDNAs were digested with the *Rsa*I restriction enzyme and subtractive hybridization was carried out using the CLONTECH PCR-Select cDNA Subtraction kit (BD Biosciences) following the manufacturer's instructions. Subtracted cDNA fragments were PCR amplified with primers binding to the adapters and cloned into the pGEM-T easy vector (Promega). *Escherichia coli* XL-1blu competent cells (Stratagene) were transformed and plated onto selective medium following the manufacturer's instructions. After plating, clones were picked into microtiter plates containing antibiotic and glycerol, grown overnight, and stored at −80°C. Colonies were analyzed by PCR amplification in 30 μL reaction volume containing 0.5 units of REDTaq polymerase (Sigma), 125 μM dNTP, and 0.5 μM each plasmid primer (T7 and SP6; Promega). Amplification consisted of an initial denaturation step for 3 min at 95°C; 35 cycles with annealing for 1 min at 55°C and 1 min 30 s at 72°C; and a final extension for 7 min at 72°C. PCR products were separated on 1.2% (w/v) agarose gels.

EST Sequencing and Analysis

One hundred and thirty-one randomly chosen SSH clones were sequenced by GeneLab after plasmid purification with QIAprep Spin Miniprep kit (Qiagen). cDNA sequence analyses were performed with Sequencer (Gene Codes). BLASTX and TBLASTX searches were carried out, respectively, in the NCBI database and the TIGR MtGI database to identify similarities on the amino acid sequences (Supplemental Table S1). Functional annotation was performed using the annot8r_BLAST2GO program (www.geneontology.org; Supplemental Fig. S1). Further analyses were performed to better characterize 15 selected genes (see below). Sequences were translated and BLASTP analyzed in the NCBI database to assess similarities to plant proteins and the presence of conserved functional domains (Supplemental Table S2). Motif scanning was carried out to find known motifs occurring in each protein sequence (http://myhits.isb-sib.ch/cgi-bin/motif_scan).

Reverse Northern Hybridization of SSH Clones

cDNA inserts from all SSH clones were amplified by PCR as described above and analyzed by dot blot reverse northern hybridizations. Briefly, amplification products were spotted in duplicate on Hybond-N+ nylon filters (Amersham) by capillary blotting and fixed under UV light (70,000 J cm^{-2}). Two identical sets of membranes were prepared for each set of clones and hybridized with digoxygenin (DIG)-labeled cDNA probes obtained from inoculated (stage 1) and corresponding control GFP-HDEL transformed wild-type roots different from those used to set up the SSH library. Probes were synthesized according to SMART-cDNA amplification technology using a dNTP mixture containing dig11-dUTP alkali labile (Roche).

Intensity of labeled cDNA probes was determined according to Dig High Prime DNA Labeling and Detection Starter Kit 2 (Roche). Membranes were hybridized with probes overnight at 68°C with a standard buffer (5× SSC; 0.1% SLS; 0.02% SDS; 1% blocking reagent). Detection was performed using CDP-Star ready-to-use substrate following the manufacturer's instructions (Roche). The chemiluminescence was captured with the VersaDoc imaging system (Bio-Rad).

EST-Specific Primer Pair Design and PCR Amplification on Genomic DNA

Specific primer pairs were designed for 15 genes selected from the SSH library (Table I). Primers were also assessed for the constitutively expressed control gene *GAPDH* (glyceraldehyde phosphate dehydrogenase), which was selected as housekeeping gene (Brechenmacher et al., 2004), and for a second set of targeted genes, which were chosen for expression analysis (Table I). Criteria for primer selection were as follows: annealing temperature ranging between 55°C and 65°C, primer lengths between 17 and 25 bp, and amplification products between 100 bp and 200 bp. The primer pair described by Levy et al. (2004) was used for *DMI3*. All the primers were tested by PCR experiments on genomic DNA of *G. margarita* to exclude cross-hybridization with fungal templates. PCR reactions were carried out using 100 ng of genomic DNA in 25 μL reaction volume containing 0.5 units of REDTaq polymerase (Sigma), 125 μM dNTP, and 0.5 μM each specific primer pair. The PCR program was as follows: 95°C for 3 min (1 cycle), 92°C for 30 s, 30 s annealing at the temperatures indicated in Table I, 72°C for 45 s (40 cycles), and 72°C for 5 min (1 cycle). Amplification products were separated on 1.5% (w/v) agarose gels.

Targeted Sequence Cloning and Analysis

The cDNA from noninoculated *M. truncatula* roots was used as a template to amplify targeted sequences chosen for expression profile analysis (Table I), in addition to the ones selected from the SSH library. PCR reactions were carried out in a final volume of 50 μL containing 200 μM each dNTP, 1 μM each primer, 50 to 100 ng of cDNA, and 2 units of REDTaq DNA polymerase (Sigma). The PCR program was as follows: 95°C for 3 min (1 cycle), 92°C for 45 s, 45 s annealing at the temperatures indicated in Table I, 72°C for 45 s (30 cycles), and 72°C for 5 min (1 cycle; according to Lanfranco et al., 2005). PCR products were separated on 1.2% to 2% (w/v) agarose gels and visualized by ethidium bromide staining. There after PCR products were extracted and purified from agarose gels using the QIAEX II gel extraction kit (Qiagen), directly cloned into the pGEM-T vector (Promega), and sequenced as described above. cDNA sequences were BLASTN analyzed.

Real-Time RT-PCR

For real-time RT-PCR analysis, RNA was obtained and checked from a different set of inoculated and noninoculated root segments collected from GFP-HDEL transformed wild-type roots during stages 1 and 2 and from GFP-HDEL transformed *dmi3-1* during stage 1, as described above. To obtain cDNAs, RT reactions were performed with random primers, following the manufacturer's instructions, using SuperScript II reverse transcriptase (Invitrogen Life Technologies). At least two separate RT reactions were performed for each RNA preparation. cDNAs were precipitated with ethanol and sodium acetate (3 M), resuspended in 100 μL of distilled water, and tested in PCR experiments with ribosomal primers NS1 and NS2 (White et al., 1990). Real-time analysis was carried out in a final volume of 20 μL containing 10 μL of 2× iQ SYBR Green Supermix (Bio-Rad; 100 mM KCl, 40 mM Tris-HCl, pH 8.4, 0.4 mM dNTPs, 50 units/mL iTaq DNA polymerase, 6 mM $MgCl_2$, 20 nM SYBR Green I, 20 nM fluorescein), 0.3 mM each oligonucleotide, and an appropriate amount of cDNAs. The following program was run: 95°C for 3 min (1 cycle) and 95°C for 15 s, and 30 s at the annealing temperatures indicated in Table I (50 cycles) in an iCycler iQ real-time PCR detection system (Bio-Rad). Data were analyzed with iCycler software. A melting curve (55°C–95°C with a heating rate of 0.5°C per 10 s and continuous fluorescence measurement) was generated at the end of every run to ensure specificity of the amplified product (Ririe et al., 1997). Melting curves were analyzed after amplification reactions and single amplification products were present in all reactions.

Standard curves were obtained using recombinant plasmids containing the sequence. Real-time PCR reactions were carried out in triplicate and only comparative threshold cycle (Ct) values leading to a Ct mean with a SD below 0.2 were considered. The Ct method (Rasmussen, 2001) was used to calculate relative gene expression levels with *gapdh* as a housekeeping gene for normalization of candidate gene expression levels, while noninoculated root explants were taken as a reference sample. The ratio between relative expression level of each gene in inoculated and noninoculated root pieces has been calculated separately during stages 1 and 2. A ratio of 1 indicates no difference between inoculated and noninoculated samples (Gao et al., 2004). We arbitrarily chose a 2-fold expression level to assess transcript up-regulation. Statistical analysis was performed using one-way ANOVA test ($P < 0.05$).

In Situ Hybridization

Sample Fixation and Embedding

Inoculated and noninoculated GFP-HDEL transformed wild-type roots were fixed in 4% paraformaldehyde in PBS (phosphate buffered saline: 130 mM NaCl; 7 mM Na_2HPO_4; 3 mM NaH_2PO_4, pH 7.4) overnight at 4°C. For the first 15 to 30 min, samples were fixed under vacuum to facilitate infiltration with the fixative. Thereafter, fixative solution was removed by washing in saline solution (150 mM NaCl) for 15 min at room temperature. The tissue was dehydrated in successive steps, each of 30 to 60 min duration, in solutions (in 150 mM NaCl) of 30%, 50%, 70%, 80%, 95%, and 100% ethanol and 100% xylene. Finally, the samples were embedded in paraffin wax (Paraplast plus; Sigma) at 60°C. Sections of 7 to 8 μm were then transferred to slides treated with 100 μg/mL poly-L-Lys (Sigma) and dried on a warm plate at 40°C overnight.

Preparation of Riboprobes

DIG-labeled RNA probes were synthesized starting with 1 μg of linearized template (Langdale, 1993). DIG-labeled riboprobes (antisense and sense probes) were produced with DIG-UTP by in vitro transcription using the pGEM-T Sp6 and T7 promoters according to the manufacturer's protocol (RNA-labeling kit; Roche).

In Situ Hybridization and Detection

The sections were treated as follows: deparaffinized in Neoclear, rehydrated through an ethanol series, treated with 0.2 M HCl for 20 min, washed in sterile water for 5 min, incubated in 2× SSC for 10 min, washed in sterile water for 5 min, incubated with proteinase K (1 μg/mL in 100 mM Tris-HCl, pH 8.0, 50 mM EDTA; Roche) at 37°C for 30 min, washed briefly in PBS, and then treated with 0.2% Gly in PBS for 5 min. After two rinses in PBS, slides were incubated in 4% paraformaldehyde in PBS for 20 min, washed in PBS (2 × 5 min), and then dehydrated in an ethanol series from 30% to 100%. Hybridizations were carried out overnight at 55°C with denatured DIG-labeled RNA probes in 50% formamide, 6× SSC, 3% SDS, 100 μg/mL tRNA, 100 μg/mL poly A. Slides were then washed twice in 1× SSC, 0.1% SDS at room temperature and rinsed with 0.2× SSC, 0.1% SDS at 55°C (2 × 10 min). After rinsing with 2× SSC for 5 min at room temperature, the nonspecifically bound DIG-labeled probe was removed by incubating in 10 μg/mL RNase A in 2× SSC at 37°C for 30 min. Slides were then rinsed twice in 2× SSC before proceeding to the next stage. The hybridized probe was detected using an alkaline phosphatase antibody conjugate (Roche). After rinsing in TBS (100 mM Tris-HCl, pH 7.5, 400 mM NaCl) for 5 min, slides were treated with 0.5% blocking reagent in TBS for 1 h, incubated for 2 h with the anti-DIG alkaline phosphatase conjugate diluted 1:500 in 0.5% BSA Fraction V in TBS, and then washed in TBS (3 × 5 min). Color development was carried out according to Torres et al. (1995). The color reaction was stopped by washing in distilled water, and the sections were then dehydrated through an ethanol series, deparaffinized in Neoclear, and mounted in Neomount (Merck).

EST data from this article can be found in the NCBI (or EMBL) database under accession numbers EC366174 to EC366280.

Supplemental Data

The following materials are available in the online version of this article.

Supplemental Figure S1. Clusters of genes identified in roots as differentially expressed upon *G. margarita* inoculation (stage 1).

Supplemental Figure S2. Transcript accumulation of selected sequences in *M. truncatula* roots inoculated with *G. margarita* (stages 1 and 2).

Supplemental Table S1. SSH sequences differentially expressed in *M. truncatula* roots during *G. margarita* appressorium formation (stage 1).

Supplemental Table S2. BLASTP similarities and conserved functional domains for *M. truncatula* selected sequences.

ACKNOWLEDGMENTS

We thank David Barker and Mireille Chabaud for kindly providing *M. truncatula* transformed roots, Stefano Ghignone for his support in sequence analysis, Pino Luciano for BIOANALYZER assays, and Daniel J. Cosgrove for his help with Exp-like sequence.

Received February 13, 2007; accepted April 13, 2007; published April 27, 2007.

LITERATURE CITED

Amiour N, Recorbet G, Robert F, Gianinazzi S, Dumas-Gaudot E (2006) Mutations in DMI3 and SUNN modify the appressorium-responsive root proteome in arbuscular mycorrhiza. Mol Plant Microbe Interact **19:** 988–997

Balestrini R, Bonfante P (2005) The interface compartment in arbuscular mycorrhizae: a special type of plant cell wall? Plant Biosyst **139:** 8–15

Balestrini R, Cosgrove DJ, Bonfante P (2005) Differential location of alpha-expansin proteins during the accommodation of root cells to an arbuscular mycorrhizal fungus. Planta **220:** 889–899

Balestrini R, Hahn MG, Faccio A, Mendgen K, Bonfante P (1996) Differential localization of carbohydrate epitopes in plant cell walls in the presence and absence of arbuscular mycorrhizal fungi. Plant Physiol **111:** 203–213

Balestrini R, Romera C, Puigdomenech P, Bonfante P (1994) Location of a cell-wall hydroxyproline-rich glycoprotein, cellulose and β-1,3-glucans in apical and differentiated regions of maize mycorrhizal roots. Planta **195:** 201–209

Bonfante P (1984) Anatomy and morphology. *In* CL Powell, DJ Bagyaraj, eds, V. A. Mycorrhizas. CRC Press, Boca Raton, FL, pp 5–33

Bonfante P, Genre A, Faccio A, Martini I, Schauser L, Stougaard J, Webb J, Parniske M (2000) The *Lotus japonicus LjSym4* gene is required for the successful symbiotic infection of root epidermal cells. Mol Plant Microbe Interact **13:** 1109–1120

Bonfante P, Perotto S (1995) Strategies of arbuscular mycorrhizal fungi when infecting host plants. Tansley Review No. 82. New Phytol **130:** 3–21

Brechenmacher L, Weidmann S, van Tuinen D, Chatagnier O, Gianinazzi S, Franken P, Gianinazzi-Pearson V (2004) Expression profiling of up-regulated plant and fungal genes in early and late stages of *Medicago truncatula-Glomus mosseae* interactions. Mycorrhiza **14:** 253–262

Cappellazzo G, Lanfranco L, Bonfante P (2007) A limiting source of organic nitrogen induces specific transcriptional responses in the extraradical structures of the endomycorrhizal fungus *Glomus intraradices*. Curr Genet **51:** 59–70

Chabaud M, Venard C, Defaux-Petras A, Bécard G, Barker DG (2002) Targeted inoculation of *Medicago truncatula* in vitro root cultures reveals MtENOD11 expression during early stages of interaction by arbuscular mycorrhizal fungi. New Phytol **156:** 265–273

Dangl JL, Jones JDG (2001) Plant pathogens and integrated defense responses to infection. Nature **411:** 826–833

Diatchenko L, Lau YF, Campbell AP, Chenchik A, Moqadam F, Huang B, Lukyanov S, Lukyanov K, Gurskaya N, Sverdlov ED, et al (1996) Suppression subtractive hybridization: a method for generating differentially regulated or tissue-specific cDNA probes and libraries. Proc Natl Acad Sci USA **93:** 6025–6030

Gal TZ, Aussenberg ER, Burdman S, Kapulnik Y, Koltai H (2006) Expression of a plant expansin is involved in the establishment of root knot nematode parasitism in tomato. Planta **224:** 155–162

Gao LL, Knogge W, Delp G, Smith FA, Smith SE (2004) Expression patterns of defense-related genes in different types of arbuscular mycorrhizal development in wild-type and mycorrhiza-defective mutant tomato. Mol Plant Microbe Interact **17:** 1103–1113

Genre A, Bonfante P (2002) Epidermal cells of a symbiosis-defective mutant of *Lotus japonicus* show altered cytoskeleton organisation in the presence of a mycorrhizal fungus. Protoplasma **219:** 43–50

Genre A, Bonfante P (2005) Building a mycorrhizal cell: how to reach compatibility between plants and arbuscular mycorrhizal fungi. J Plant Interact **1:** 3–13

Genre A, Chabaud M, Timmers T, Bonfante P, Baker GD (2005) Arbuscular mycorrhizal fungi elicit a novel intracellular apparatus in *Medicago truncatula* root epidermal cells before infection. Plant Cell **17:** 3489–3499

Giordano W, Hirsch AM (2004) The expression of *MaEXP1*, a *Melilotus alba* expansin gene, is upregulated during the sweetclover-*Sinorhizobium meliloti* interaction. Mol Plant Microbe Interact **17:** 613–622

Guimil S, Chang H, Zhu T, Sesma A, Osbourn A, Roux C, Ioannidis V, Oakeley EJ, Docquier M, Descombes P, et al (2005) Comparative transcriptomics of rice reveals an ancient pattern of response to microbial colonization. Proc Natl Acad Sci USA **102:** 8066–8070

Haseloff J, Siemering RK, Prasher DC, Hodge S (1997) Removal of a cryptic intron and subcellular localization of green fluorescent protein are required to mark transgenic *Arabidopsis* plants brightly. Proc Natl Acad Sci USA **94:** 2122–2127

Hohnjec N, Vieweg MF, Puhler A, Becker A, Küster H (2005) Overlaps in the transcriptional profiles of *Medicago truncatula* roots inoculated with two different glomus fungi provide insights into the genetic program activated during arbuscular mycorrhiza. Plant Physiol **137:** 1283–1301

Journet EP, van Tuinen D, Gouzy J, Crespeau H, Carreau V, Farmer MJ, Niebel A, Schiex T, Jaillon O, Chatagnier O, et al (2002) Exploring root symbiotic programs in the model legume *Medicago truncatula* using EST analysis. Nucleic Acids Res **30:** 5579–5592

Karandashov V, Bucher M (2005) Symbiotic phosphate transport in arbuscular mycorrhizas. Trends Plant Sci **10:** 22–29

Kistner C, Winzer T, Pitzschke A, Mulder L, Sato S, Kaneko T, Tabata S, Sandal N, Stougaard J, Webb J, et al (2005) Seven *Lotus japonicus* genes required for transcriptional reprogramming of the root during fungal and bacterial symbiosis. Plant Cell **17:** 2217–2229

Küster H, Vieweg MF, Manthey K, Baier MC, Hohnjec N, Perlick AM (2007) Identification and expression regulation of symbiotically activated legume genes. Phytochemistry **68:** 8–18

Lanfranco L, Novero M, Bonfante P (2005) The mycorrhizal fungus *Gigaspora margarita* possesses a CuZn superoxide dismutase that is up-regulated during symbiosis with legume hosts. Plant Physiol **137:** 1319–1330

Langdale JA (1993) *In situ* hybridization. *In* M Freeling, V Walbot, eds, The Maize Handbook. Springer, Berlin, pp 165–180

Lange J, Xie Z-P, Broughton WJ, Vögeli-Lange R, Boller T (1999) A gene encoding a receptor-like protein kinase in the roots of common bean is differentially regulated in response to pathogens, symbionts and nodulation factors. Plant Sci **142:** 133–145

Levy J, Bres C, Geurts R, Chalhoub B, Kulikova O, Duc G, Journet EP, Ane JM, Lauber E, Bisseling T, et al (2004) A putative Ca2+ and calmodulin-dependant protein kinase required for bacterial and fungal symbioses. Science **303:** 1361–1364

Liu J, Blaylock LA, Endre G, Cho J, Town CD, VandenBosch KA, Harrison MJ (2003) Transcript profiling coupled with spatial expression analyses reveals genes involved in distinct developmental stages of an arbuscular mycorrhizal symbiosis. Plant Cell **15:** 2106–2123

Lohse S, Schliemann W, Ammer C, Kopka J, Strack D, Fester T (2005) Organization and metabolism of plastids and mitochondria in arbuscular mycorrhizal roots of *Medicago truncatula*. Plant Physiol **139:** 329–340

Manthey K, Krajinski F, Hohnjec N, Firnhaber C, Pühler A, Perlick AM, Küster H (2004) Transcriptome profiling in root nodules and arbuscular mycorrhiza identifies a collection of novel genes induced during *Medicago truncatula* root endosymbioses. Mol Plant Microbe Interact **17:** 1063–1077

Massoumou M, van Tuinen D, Chatagnier O, Arnould C, Brechenmacher L, Sanchez L, Selim S, Gianinazzi S, Gianinazzi-Pearson V (2007) *Medicago truncatula* gene responses specific to arbuscular mycorrhiza interactions with different species and genera of Glomeromycota. Mycorrhiza **17:** 223–234

Navazio L, Moscatiello R, Genre A, Novero M, Baldan B, Bonfante P, Mariani P (2007) A diffusible signal from arbuscular mycorrhizal fungi elicits a transient cytosolic calcium elevation in host plant cells. Plant Physiol **144:** 673–681

Oldroyd GED, Harrison MJ, Udvardi M (2005) Peace talks and trade deals. Keys to long-term harmony in legume-microbe symbioses. Plant Physiol **137:** 1205–1210

Parniske M (2004) Molecular genetics of the arbuscular mycorrhizal symbiosis. Curr Opin Plant Biol **7:** 414–421

Rae AL, Bonfante-Fasolo P, Brewin NJ (1992) Structure and growth of infection threads in the legume symbiosis with *Rhizobium leguminosarum*. Plant J **2:** 385–395

Rasmussen R (2001) Quantification on the LightCycler. *In* S Mener, C Wittwer, K Nakagawara, eds, Rapid Cycle Real-Time PCR: Methods and Applications. Springer Press, Heidelberg, pp 21–34

Ririe KM, Rasmussen RP, Wittwer CT (1997) Product differentiation by analysis of DNA melting curves during the polymerase chain reaction. Anal Biochem **245:** 154–160

Rowland O, Ludwig AA, Merrick CJ, Baillieul F, Tracy FE, Durrant WE, Fritz-Laylin L, Nekrasov V, Sjölander K, Yoshioka H, et al (2005) Functional analysis of *Avr9/Cf-9* rapidly elicited genes identifies a protein kinase, ACIK1, that is essential for full Cf-9-dependent disease resistance in tomato. Plant Cell **17:** 295–310

Sagan M, de Larambergue H, Morandi D (1998) Genetic analysis of symbiosis mutants in *Medicago truncatula*. *In* C Elmerich, A Kondorosi, WE Newton, eds, Biological Nitrogen Fixation for the 21st Century. Kluwer Academic Publishers, Dordrecht, The Netherlands, pp 317–318

Sampedro J, Cosgrove DJ (2005) Protein family review: the expansin superfamily. Genome Biol **6:** 242

Schüßler A, Schwarzott D, Walker C (2001) A new fungal phylum, the Glomeromycota: phylogeny and evolution. Mycol Res **105:** 1413–1421

Smith SE, Barker SJ, Zhu YG (2006) Fast moves in arbuscular mycorrhizal symbiotic signalling. Trends Plant Sci **11:** 369–371

Smith SE, Read DJ (1997) Mycorrhizal Symbiosis. Academic Press, London

Tirichine L, Imaizumi-Anraku H, Yoshida S, Murakami Y, Madsen L, Miwa H, Nakagawa T, Sandal N, Albrektsen AS, Kawaguchi M, et al (2006) Deregulation of a Ca2+/calmodulin-dependent kinase leads to spontaneous nodule development. Nature **441:** 1153–1156

Torres MA, Rigau J, Puigdomenech P, Stiefel V (1995) Specific distribution of mRNAs in maize growing pollen tubes observed by whole-mount *in situ* hybridization with non-radioactive probes. Plant J **8:** 317–321

Vieweg MF, Fruhling M, Quandt HJ, Heim U, Baumlein H, Puhler A, Küster H, Perlick AM (2004) The promoter of the *Vicia faba* L. leghemoglobin gene *VfLb29* is specifically activated in the infected cells of root nodules and in the arbuscule-containing cells of mycorrhizal roots from different legume and non legume plants. Mol Plant Microbe Interact **17:** 62–69

Vieweg MF, Hohnjec N, Kuster H (2005) Two genes encoding different truncated haemoglobins are regulated during root nodule and arbuscular mycorrhiza symbioses of *Medicago truncatula*. Planta **220:** 757–766

Weidmann S, Sanchez L, Descombin J, Chatagnier O, Gianinazzi S, Gianinazzi-Pearson V (2004) Fungal elicitation of signal transduction-related plant genes precedes mycorrhiza establishment and requires the *dmi3* gene in *Medicago truncatula*. Mol Plant Microbe Interact **17:** 1385–1393

White TJ, Bruns T, Lee S, Taylor J (1990) Amplification and direct sequencing of fungal ribosomal RNA genes for phylogenetics. *In* MA Innis, DH Gelfand, JJ Sninsky, TJ White, eds, PCR Protocols. A Guide to Methods and Applications. Academic Press, San Diego, pp 315–322

Wulf A, Manthey K, Doll J, Perlick AM, Linke B, Bekel T, Meyer F, Franken P, Küster H, Krajinski F (2003) Transcriptional changes in response to arbuscular mycorrhiza development in the model plant *Medicago truncatula*. Mol Plant Microbe Interact **16:** 306–314